Enseign. Math. (2) 70 (2024), 479–497
DOI 10.4171/LEM/1062

Hexagonal pencils of cubic plane curves

Joel Langer and Jeremy Wall

Abstract. This expository paper considers real cubic plane curves as combinations $C = a_1T_1 + a_2T_2$ of two real triangles meeting in nine distinct points. Our study of *hexagonal pencils*, defined by C with parameters $a_i \in \mathbb{R}$, picks up on some themes of a recent paper on cubics by Bonifant and Milnor (2017).

Mathematics Subject Classification 2020: 14H50 (primary); 14C21, 14N10, 34A26 (secondary).

Keywords: cubic plane curve, pencil, singular foliation, j-invariant, Kodaira fiber.

1. Introduction

A regular pencil of real cubics $F : \alpha G + \beta H$ may have any number of singular curves in the range $0 \le n \le 12$. As a foliation of $\mathbb{R}\mathrm{P}^2$, F may have any number of singularities in the range $1 \le N \le 21$ – counting base points (common to all curves in F) and isolated curve singularities belonging to a unique curve.

Such results were obtained in [7] in the course of investigating *decomposable* pencils

$$F : \alpha G_1G_2G_3 + \beta H_1H_2H_3$$

(defined by six distinct lines), for which the corresponding numbers are $2 \le n \le 8$ and $2 \le N \le 21$. The most interesting examples tend to be *hexagonal* pencils (or *hex* pencils), defined by two real triangles T_1, T_2 meeting in nine distinct points (the generic case among $\mathbb{R}$-*decomposable* pencils). Hexagonal pencils cover the ranges $3 \le n \le 8$ and $16 \le N \le 21$.

While hex pencils are quite special, they are well suited for representing real cubics. In addition to demonstrating this here, we intend to provide an overview of the topology of hex pencils as a class of *pencil foliations* of $\mathbb{R}\mathrm{P}^2$.

To begin, we construct a family of hex pencils with symmetry of the dihedral group D_3, each of which represents all smooth real cubics (Theorem 4.2). Such a pencil will be called *full*, while a *perfect* pencil represents each smooth, irreducible

real cubic exactly *once*. In particular, the *Hessian pencil*

$$\mathcal{H} : \alpha(x^3 + y^3 + z^3) + \beta xyz$$

is a perfect pencil. Here we are paraphrasing a result from [2] (Theorem 2.1, below), which assigns to $\mathcal{H}$ a leading role in the theory of real cubics. (The more famous appearance of $\mathcal{H}$ in the complex theory also requires the j-invariant to effectively factor out a tetrahedral group of symmetries of $\mathcal{H}$.)

Thus we obtain full hex pencils, essentially, by comparison with $\mathcal{H}$. But when it comes to representing *singular* cubics, hex pencils are more versatile. While the only singular cubics in $\mathcal{H}$ are triangles, a sufficient set of hex pencils will be constructed here to establish (Theorem 5.4): A real cubic belongs to a hex pencil if and only if it has no repeated line, imaginary line-pair, or imaginary conic (nomenclature as in Proposition 5.1).

Further, we proceed to identify all (real and complex) singular cubics in many additional hex pencils, and thus obtain a fuller picture of their range of topological behavior. This last part of the paper is more open-ended, but aims towards a classification of hex pencil foliations of $\mathbb{R}\mathrm{P}^2$.

Table 2 contains the following topological data for the singular cubics in each of the 15 hex pencils shown in Figure 7:

(1) The Euler number $\chi(C_{\mathbb{R}})$ of the topological subspace $C_{\mathbb{R}} \subset \mathbb{R}\mathrm{P}^2$;

(2) The Euler number $\chi(C_{\mathbb{C}})$ of $C_{\mathbb{C}} \subset \mathbb{C}\mathrm{P}^2$;

(3) The corresponding Kodaira fiber type in the associated rational elliptic surface, obtained by blowing up at the 9 base points of the pencil.

We need not dwell on the latter, since no subtleties arise here. In fact, only 6 of the 20 possible singular fiber types occur for hex pencils (see Table 1). This is partly due to all base points being *simple* (that is, transverse intersections), and also due to the lack of repeated components (Proposition 5.2). The upshot is that for singular cubics in hex pencils, Euler numbers (1) and (2) determine fiber type (3).

On the other hand, we wish to compare the *fiber configurations* $\mathcal{K}$ in Table 2 against the list of 279 configurations which occur in rational elliptic surfaces [9]. This will provide one measure of completeness of our current list of topologically distinct hex pencils. It turns out we are still missing 3 of the 17 *hex-like* configurations, which may or may not actually occur for hex pencils. Thus, our paper ends with an open question.

The paper is organized as follows. In Section 2, we review some of the relevant facts about $\mathcal{H}$, the j-invariant, and the *k-invariant* (following [2]). In Section 3, we display an equivalent pencil $\widetilde{\mathcal{H}}$, with symmetry of the dihedral group D_3. The pencil $\widetilde{\mathcal{H}}$

leads to the D_3-*normal form* (almost the *canonical position* of [2]), and corresponding formulas for j and k. In Section 4, the D_3-normal form is used to construct full hex pencils.

A number of types of singular real cubics (and the non-singular, reducible type) appear in the D_3-symmetric hex pencils of Section 4. The remainder require special hex pencils with D_2-symmetry or just reflection symmetry, and are treated in Section 5.

We begin Section 6 by explaining the basic constraints on the Euler numbers of singular curves in a hex pencil of cubics. (For general regular pencils, one needs to consider corresponding *fibers*.) In the real setting, $\sum \chi(C^i_{\mathbb{R}}) = -8$; in the complex case, $\sum \chi(C^i_{\mathbb{C}}) = 12$. Although the blow up process provides topological explanations for both, alternative interpretations work very well for hex pencils.

In the real case, we apply the Poincaré–Hopf theorem for the sum of indices of a line field. For the complex case, we consider the 12th-degree *discriminant form* $\Delta(\alpha, \beta)$, which vanishes precisely when $C = \alpha G + \beta H$ is a singular cubic. As it turns out, the multiplicity of the root $(\alpha : \beta)$ is invariably $\chi(C_{\mathbb{C}})$! (Not so for regular pencils in general.) This explains not only the sum $\sum \chi(C^i_{\mathbb{C}}) = 12$, but also accounts for the utility of Δ as a general tool for identifying types of singular cubics in a hex pencil. The remainder of Section 6 is a compilation of examples based on Δ (we omit computational details).

2. The Hessian pencil of cubics in real and complex settings

In this section, we briefly recall the main features of the Hessian pencil of cubics, $\mathcal{H} : \alpha(x^3 + y^3 + z^3) + \beta xyz$, and how it may be used to describe the equivalence classes of non-singular cubics with respect to both real and complex projective transformations. (Further background may be found in [1–3, 5].)

We are especially interested in the Hessian pencil for real values of α, β. Figure 1 (A) shows $\mathcal{H}$ in the x, y-plane and Figure 1 (B) shows $\mathcal{H}$ in the disk model $\mathbb{D}^2 \simeq \mathbb{R}\mathrm{P}^2$, where ideal points become visible (as antipodal pairs on the green circle).

But first we describe the pencil in $\mathbb{C}\mathrm{P}^2$, with parameter $(\alpha : \beta) \in \mathbb{C}\mathrm{P}^1$. It is convenient to write $-3k = \beta/\alpha \in \widehat{\mathbb{C}}$, and express $\mathcal{H}$ and the j-invariant along $\mathcal{H}$:

$$\mathcal{H} : (x^3 + y^3 + z^3) - 3kxyz, \quad j(k) = \frac{k^3(k^3 + 8)^3}{64(k^3 - 1)^3}.$$

Then $\mathcal{H}$ degenerates to a triangle at each of the four k-values: $k = 1, e^{2\pi i/3}, e^{4\pi i/3}, \infty$. Otherwise, $\mathcal{H}$ is non-singular. We discuss the j-invariant shortly; for now we simply note that its poles are exactly the k-values where $\mathcal{H}$ becomes singular.

The *base points* of $\mathcal{H}$ are the 9 intersection points of the four triangles. These are in fact the 9 *flexes* on the Fermat cubic $F = x^3 + y^3 + z^3$; namely, the intersections

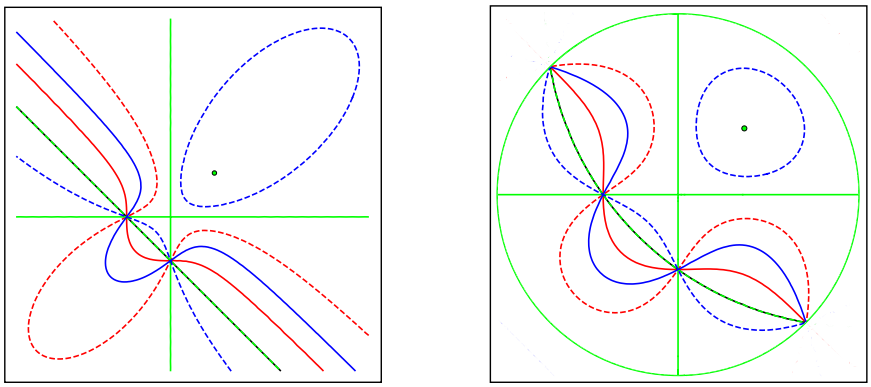

(A) (B)

FIGURE 1
(A) Real curve–pairs in the Hessian pencil $\mathcal{H}$ with $j = 0$ (red), $j = 1$ (blue), and $j = \infty$ (green); (B) view of $\mathcal{H}$ in $\mathbb{D}^2$.

of F with the cubic obtained as the Hessian $H(F) = |D^2F| = 6xyz$. The same points are likewise the 9 flexes on each of the non-singular cubics in $\mathcal{H}$.

The 9 points and 12 lines (triangular edges) form a configuration which plays a key role in the theory of cubics. That a structure this special is of general importance depends on this fact: Any non-singular cubic C in $\mathbb{C}\mathrm{P}^2$ can be put into *Hessian normal form*, that is, C is equivalent by complex projective transformations to some cubic in $\mathcal{H}$. It follows also that, up to projective equivalence in $\mathbb{C}\mathrm{P}^2$ (and projective change of parameter), $\mathcal{H}$ is the unique pencil of the form $F_G : \alpha G + \beta H(G)$, where G is a non-singular cubic.

Turning to the significance of the j-invariant: Two non-singular cubics in $\mathcal{H}$ are equivalent by complex projective transformations if and only if their k-values satisfy $j(k_1) = j(k_2)$. Thus, we want to understand the geometry of level sets of j.

To begin, the 4 poles of j may be regarded as *tetrahedral vertices*; they are permuted by a copy of the tetrahedral group $\mathcal{T} \simeq A_4$, a subgroup of the Möbius group $\mathcal{T} \subset \mathrm{PGL}(2, \mathbb{C})$. Namely, $\mathcal{T}$ is generated by the rotation $\rho(k) = e^{2\pi i/3}k$ and the involution $\eta(k) = \frac{k+2}{k-1}$ (see [2]). Further, one can verify directly that ρ and η leave j unchanged. Thus we have the remarkable fact: $j(k)$ *is an automorphic function with respect to the tetrahedral group* $\mathcal{T}$.

The upshot is that $\mathcal{T}$-orbits correspond exactly to equivalence classes of cubics in $\mathcal{H}$. For example, *face centers*, defined by $j(k) = 0$, give 4 "copies" of the *Fermat cubic* $x^3 + y^3 + z^3$; likewise *edge midpoints*, $j(k) = 1$, give 6 equivalent cubics. The 14 curves in $\mathcal{H}$ mentioned so far correspond to ramification values $j = 0, 1, \infty$. Every

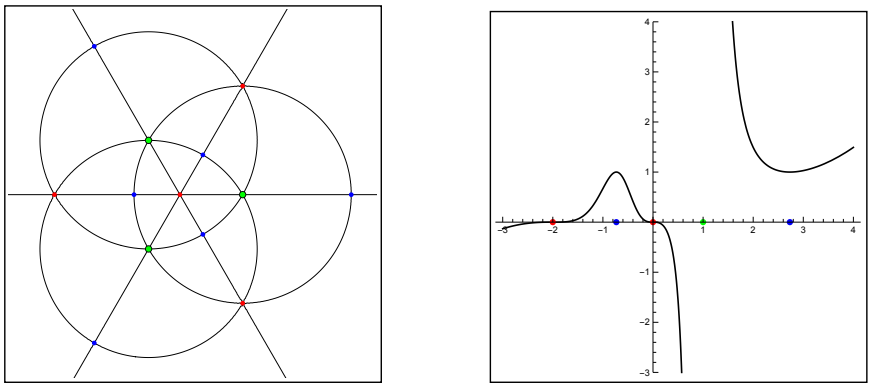

(A) (B)

FIGURE 2
Ramification points of $j(k)$ along Hessian pencil $\mathcal{H}$: (A) for $k \in \widehat{\mathbb{C}}$; (B) for $k \in \widehat{\mathbb{R}}$. (Key: $j = 0, 1, \infty \to$ red, blue, green.)

$j \neq 0, 1, \infty$ defines a $\mathcal{T}$-orbit of length 12, hence, a dozen equivalent cubics. The situation is depicted in Figure 2 (A).

Now we reconsider the Hessian pencil from the real point of view, $\mathcal{H} \subset \mathbb{R}\mathrm{P}^2$. The main features of $j(k)$ for real values of k are visible in Figure 2. The real axis in (A), and the k-axis in (B), may be identified with the cross section of a tetrahedron in $\mathbb{R}^3$ cut out by a plane of reflection symmetry. More precisely, the cross section is parametrized by a copy of the extended real line $\widehat{\mathbb{R}}$.

There are 6 special values $k \in \widehat{\mathbb{R}}$ – two for each color (red, blue, green), paired by the involution $\eta(k) = \frac{k+2}{k-1}$. In fact, j maps all of $\widehat{\mathbb{R}}$ onto itself, two-to-one. There are triple zeros at $k = 0, -2$, triple poles at $k = 1, \infty$, and critical points at $k = 1 \pm \sqrt{3}$ (j is normalized so that $j(1 \pm \sqrt{3}) = 1$). As indicated in Figure 2 (B), j maps $(1 - \sqrt{3}, 1) \cup (1, 1 + \sqrt{3})$ injectively onto $\mathbb{R} \setminus \{1\}$; likewise for $(-\infty, 1 - \sqrt{3}) \cup (1 + \sqrt{3}, \infty)$. The latter two subsets are interchanged by η.

Although η pairs curves in $\mathcal{H}$ of the same j-value, it is important to note that the two curves are *not* equivalent in $\mathbb{R}\mathrm{P}^2$. For example, the solid blue curve in Figure 1 has one connected component, the dashed curve has two. Otherwise, paired curves have the same number of components, so topology alone does not settle things.

But the matter is definitively addressed in [2, Theorem 6.3].

Theorem 2.1. *Every smooth irreducible real cubic C is real projectively equivalent to exactly one cubic in the Hesse normal form, with $k \in (-\infty, 1) \cup (1, \infty)$. If $k < 1$, $C \subset \mathbb{R}\mathrm{P}^2$ is connected, and if $k > 1$, C has two components.*

Paraphrasing (the first part of) the theorem: *k plays the same role for real cubics as the j-invariant plays for cubics in* $\mathbb{C}\mathrm{P}^2$. Thus, we will sometimes refer to k as *the k-invariant* to underscore this fact. (We use the same letter k as in [2], where the authors remark that they were unable to find their result in the literature.)

3. D_3-normal form for real cubics

Each curve in the Hessian pencil $\mathcal{H}$ has six real projective symmetries given by permutations of coordinates x, y, z. These fix $e_0 = (1 : 1 : 1)$ and permute the three real flexes

$$(-1 : 0 : 1), \quad (0 : -1 : 1), \quad (-1 : 1 : 0)$$

of the smooth curves in $\mathcal{H}$. It is useful to note that the symmetries also permute the vertices

$$e_1 = (1 : 0 : 0), \quad e_2 = (0 : 1 : 0), \quad e_3 = (0 : 0 : 1)$$

of the triangle $\triangle = \mathcal{H}|_{k=\infty} = xyz$.

The above suggests how to turn the Hessian pencil into an equivalent pencil with the geometrically familiar symmetry of the dihedral group $D_3 \simeq S_3$; see Figure 3. A unique real projective transformation Φ maps the four points $\{e_i\}$ to vertices of an equilateral triangle

$$v_1 = (\sqrt{3} : 1 : 1), \quad v_2 = (-\sqrt{3} : 1 : 1), \quad v_3 = (0 : -2 : 1)$$

and its centroid $v_0 = (0 : 0 : 1)$ (both 4-tuples being in general position). Namely, Φ and its inverse $\phi = \Phi^{-1}$ are given by:

$$\Phi : X = \sqrt{3}x - \sqrt{3}y, \quad Y = x + y - 2z, \quad Z = x + y + z;$$

$$\phi : x = \sqrt{3}X + Y + 2Z, \quad y = -\sqrt{3}X + Y + 2Z, \quad z = -2Y + 2Z.$$

Note Φ takes the above flexes to ideal points $(1 : \pm\sqrt{3} : 0)$, $(1 : 0 : 0)$.

Substitution by ϕ in $\mathcal{H}$ (and reverting to lower case) gives the equivalent pencil:

$$\widetilde{\mathcal{H}} : (k-1)(3x^2y - y^3 + 4z^3) - 3(k+2)(x^2 + y^2)z.$$

The cubics in the pencil are now in *canonical position*; see [2, Remark 6.9] (except for the suggested z-rescaling, which would not have preserved $\widetilde{\mathcal{H}}$ as a pencil).

Remark 3.1. We could have written $\widetilde{\mathcal{H}}$ (less compactly) in the form $\widetilde{\mathcal{H}} : F + k\triangle$, with F (solid red curve in Figure 3) the Φ-image of the Fermat cubic $x^3 + y^3 + z^3$, and $\triangle$ the (green) equilateral triangle. Instead, $\widetilde{\mathcal{H}} : \alpha F^* + \beta\odot$ is generated by $F^* = 3x^2y - y^3 + 4z^3$ (dashed red curve) satisfying $j(F^*) = j(F) = 0$, and the *conjugate triangle* $\odot = -3(x^2 + y^2)z$. The real locus of $\odot$ (ideal line and the isolated singularity at the origin) appears (dashed green) in Figure 3 (B).

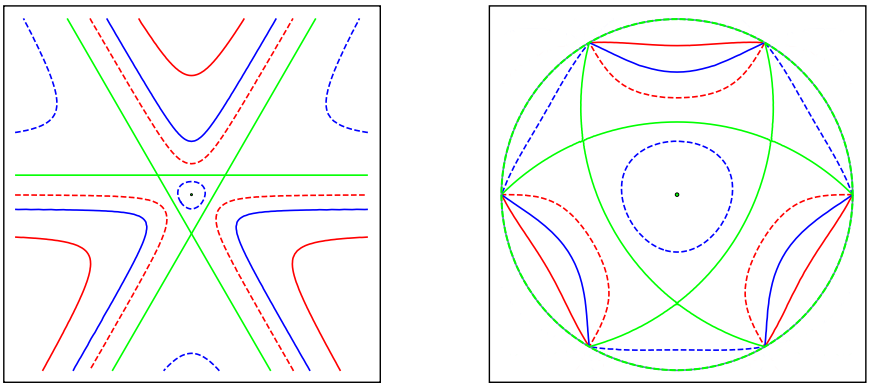

(A) (B)

FIGURE 3
A D_3-symmetric pencil $\widetilde{\mathcal{H}} \simeq \mathcal{H}$: (A) in $\mathbb{R}^2$; (B) in $\mathbb{D}^2$.

We note that $\widetilde{\mathcal{H}}$ is a perfect pencil, but not a hex pencil. While there are no perfect hex pencils, $\widetilde{\mathcal{H}}$ leads us closer to the construction of full hex pencils. For this purpose, it will be useful to have a redundant version of the above-mentioned *canonical position*, which we will refer to as the D_3-*normal form*:

$$\begin{aligned} T_{a,b} &= (3x^2y - y^3) - 3a(x^2+y^2)z + 4bz^3; \\ j &= \frac{(a^4+8ab)^3}{64b(a^3-b)^3}; \quad k = \eta\Big(\frac{a}{b^{1/3}}\Big). \end{aligned} \tag{3.1}$$

Here we note that the change of variable $z \mapsto b^{1/3}z$ gives an isomorphism between $\widetilde{\mathcal{H}}(k) = 0$ and $T_{a,b} = 0$ with $\eta(k) = a/b^{1/3}$. Thus,

$$j(T_{a,b}) = j(k) = j(\eta(k)) = j\Big(\frac{a}{b^{1/3}}\Big),$$

giving the formula for j in equation (3.1).

The tangents to $T = T_{a,b}$ at flexes $(1:0:0)$, $(1:\pm\sqrt{3}:0)$ form the triangle/star

$$\begin{aligned} \triangledown_a &= (3x^2y - y^3) - 3a(x^2+y^2)z + 4a^3z^3 \\ &= (y - az)(3x^2 - (y+2az)^2). \end{aligned}$$

Note that any smooth cubic C with the above flexes and D_3 symmetry has the *tangent triangle/star* (formed by the tangents at flexes) $\triangledown(C) = \triangledown_a$, for some $a \in \mathbb{R}$. (For example, a smooth cubic in $\widetilde{\mathcal{H}}$ has the tangent triangle $\triangledown_{\eta(k)}$.) Taking a non-inflection point $q \in C$, one can always choose b in equation (3.1) so that $T(q) = 0$. Then $T_{a,b}$ meets C ten times (counting each flex three times), so $C = T_{a,b}$.

Aside from $\widetilde{\mathcal{H}}$, there are other interesting pencils in D_3-normal form. For example, the pencil $P : T_{1,b}$ is the level set diagram of the affine cubic

$$p(x, y) := (3x^2y - y^3) - 3(x^2 + y^2)$$

(and the repeated ideal line z^3), which looks quite similar to $\widetilde{\mathcal{H}}$. The invariants

$$j = \frac{(1 + 8b)^3}{64b(1 - b)^3}, \quad k = \frac{1 + 2b^{1/3}}{1 - b^{1/3}}$$

indicate that P is almost a perfect pencil; it lacks only a representative of

$$F^* = 3x^2y - y^3 + 4z^3,$$

with $j = 0, k = -2$. In P, $j = 0, k = -2$ are the limiting values for the singular cubic z^3! Finally, we note that the two critical level sets of p are: $p(x, y) = -4$ (the fixed tangent triangle $\bigtriangledown_1$ for curves in P), and the acnodal cubic $p(x, y) = 0$.

Figure 4 shows several more examples of pencils in D_3-normal form. One of these will be used in the next section to prove Theorem 4.2.

4. Hex pencils in D_3-normal form

Next, we consider pencils generated by pairs of triangles of the type $\bigtriangledown_a$:

$$F_{\ell,m} : \alpha \bigtriangledown_\ell + \beta \bigtriangledown_m = (\alpha + \beta)(3x^2y - y^3) - 3(\alpha\ell + \beta m)(x^2 + y^2)z + 4(\alpha\ell^3 + \beta m^3)z^3. \tag{4.1}$$

Figure 4 shows three examples of $F_{\ell,m}$ using the disk model of the projective plane $\mathbb{D}^2 \simeq \mathbb{R}\mathrm{P}^2$ to plot the corresponding pencil foliations. The generating triangles $\bigtriangledown_\ell, \bigtriangledown_m$ are shown in red and blue; we note that their edges (lines) are represented by circular arcs in the disk model. The remaining singular or reducible curves in $F_{\ell,m}$ (colored/dashed) are explained in the proof of Theorem 4.2.

We note that the left pencil $F_{-1,1/4}$ represents the generic case of $F_{\ell,m}$, which is a hex pencil with D_3 symmetry. The middle pencil $F_{-1,1}$ is also a hex pencil; but because of its exceptional D_6 symmetry, it contains a *star* $\bigtriangledown_0$ and gives a topologically different foliation. Finally, $F_{-1,1/2}$, which is generated by one triangle inscribed in another, is *bi-triangular*. These remarks lead up to the following definition.

Definition 4.1. A *D_3-hex pencil* $F_{\ell,m}$ is given by equation (4.1), where $\ell \neq 0$ and $m = r\ell$ for real $r \neq 0, \pm 1, -2, -1/2$. (So $F_{-1,1}$ and $F_{-1,1/2}$ are not D_3-hex pencils!)

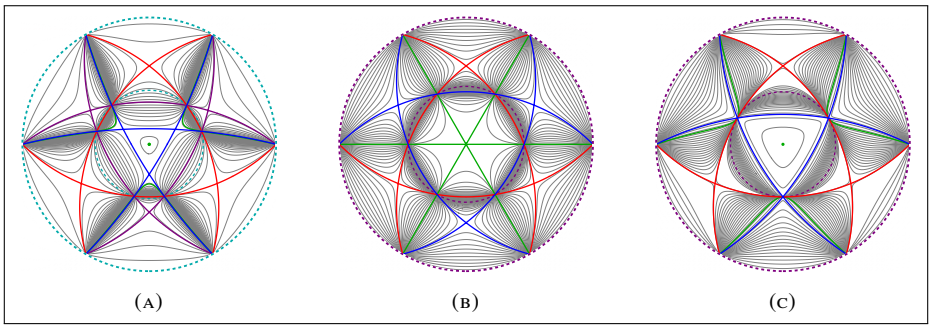

FIGURE 4
Pencils $F_{\ell,m}$ in $\mathbb{D}^2$: (A) $F_{-1,1/4}$; (B) $F_{-1,1}$; (C) $F_{-1,1/2}$.

Theorem 4.2. *There exist full hex pencils. In particular, each D_3-hex pencil $F_{\ell,m}$ contains representatives of every smooth, irreducible real cubic C.*

Proof. Let $F_{\ell,m} = F_{\ell,r\ell}$ be a D_3-hex pencil. Note that $\alpha + \beta = 0$ gives the (non-singular) reducible cubic consisting of a circle centered at the origin and the ideal line (dashed in Figure 4 (A). For all other cubics in the pencil, we can normalize by $\alpha + \beta = 1$ so that $F_{\ell,m}$ has the D_3-normal form T. Then the cube of the invariant $\eta = \eta(k)$ defines a rational function

$$f(\alpha) := \eta^3 = \frac{a^3}{b} = \frac{(\alpha\ell + \beta m)^3}{\alpha\ell^3 + \beta m^3} = \frac{((1-r)\alpha + r)^3}{(1-r^3)\alpha + r^3}.$$

Since $r \neq \pm 1$, this fraction does not reduce. In fact, $f(\alpha)$ has a triple zero at $\alpha_0 = \frac{r}{r-1}$, a simple pole at $\alpha_1 = \frac{r^3}{r^3-1}$, and a double pole at $\alpha_2 = \infty$. As a map of the extended real line to itself, f has topological degree ± 1. So f assumes every real value; but then the same must hold for its restriction to $\mathbb{R}$, since $f(\infty) = \infty$. Thus, η takes on all real values for curves in $F_{\ell,r\ell}$.

The exceptional value $\eta = 1$ ($k = \infty$) occurs for the two generating triangles ∇_m, ∇_ℓ: $f(0) = f(1) = 1$. In fact, there is always a third triangle corresponding to

$$f(\alpha) = f\Big(\frac{2r+1}{r-1}\Big) = 1$$

(purple triangle in Figure 4 (A)). Also, there is an acnodal cubic for $f(\alpha_1) = \infty$ (solid green). Counting as well the smooth, reducible cubic for $\alpha + \beta = 0$, there are thus *five* exceptional cubics in the pencil. These account for the roots of the 12th-degree *discriminant form* along the pencil (see Section 6)

$$\Delta(\alpha, \beta) = (r-1)^6\alpha^3\beta^3((r+2)\alpha + (2r+1)\beta)^3(\alpha+\beta)^2(\alpha+\beta r^3);$$

the triangles give triple roots, the circle/line gives a double root, and the acnodal cubic gives a simple root.

It follows that the rest of the pencil consists of smooth irreducible cubics corresponding to all values $\eta \neq 1, \infty$ ($k \neq \infty, 1$). So Theorem 2.1 implies that every smooth irreducible real cubic is real projectively equivalent to a curve in $F_{\ell,m}$. Since real projective transformations preserve the class of hex pencils, the second statement of the proposition follows. ∎

Remark 4.3. The hex pencil $F_{-1,1}$ shown in Figure 4 (B) is not full. For $r = -1$, a cancellation results in $f(\alpha) = (2\alpha - 1)^2$, so $F_{-1,1}$ lacks cubics with $\eta < 0$, i.e., $-2 < k < 1$; in particular, it misses cubics with $0 < j < 1$. On the other hand, $F_{-1,1}$ contains exactly two representatives of every irreducible real cubic with two connected components.

The bi-triangular pencil $F_{-1,1/2}$ (Figure 4 (C)) is full, since $f(\alpha) = \frac{(-2+3\alpha)^3}{-8+9\alpha}$ takes every real value. In fact, $F_{-1,1/2}$ represents every cubic with $k < 1$ once, and every cubic with $k > 1$ thrice!

5. Singular/reducible real cubics in hex pencils

It is well known that every cubic belongs to one of nine *geometric types* (nomenclature as in [5]): general, nodal, cuspidal, conic-plus-chord, conic-plus-tangent, triangle, three-line-type (star), two-line-type, one-line-type. The *general type* is actually the continuum of equivalence classes of non-singular cubics, while the last eight types are unique singular cubics, up to complex projective equivalence.

In the real projective setting, this list has to be expanded. For instance, one has to distinguish between *nodal* cubics, with two real tangents at the double point p, and *acnodal* cubics, with a pair of complex conjugate tangents at p.

Triangles and stars can have three real edges, or one real edge and an *imaginary line-pair* (e.g., $x^2 + y^2$). A conic-plus-chord can be *singular*, with two real double points. Or it can be *non-singular*, with complex conjugate double points; in the latter case, the conic can either be *real* (e.g., $x^2 + y^2 - z^2$), or *imaginary* (e.g., $x^2 + y^2 + z^2$). (Apologies for calling some real curves "imaginary"!)

Proposition 5.1. *The types of real cubic curves C are enumerated as follows:*

(a) *C is smooth and irreducible: $k(C) = k_0$ for exactly one $k_0 \in \mathbb{R} \setminus \{1\}$;*

(b) *C singular and irreducible: C is nodal, acnodal, or cuspidal;*

(c) *C is reducible but indecomposable: C is a conic-plus-tangent, singular conic-plus-chord, or non-singular conic-plus-chord, with real or imaginary conic;*

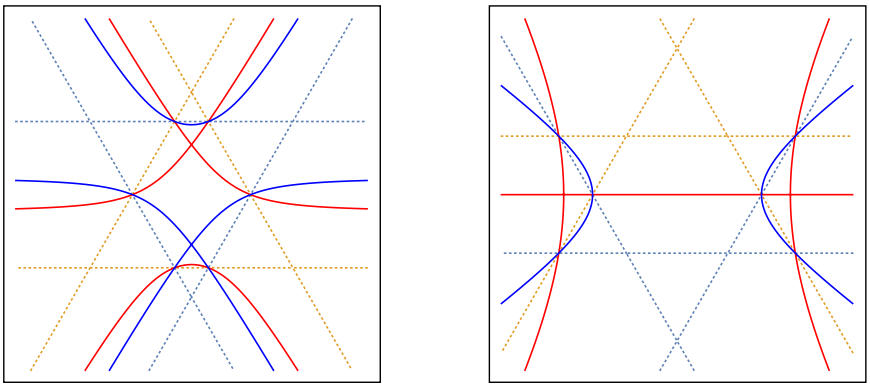

(A) (B)

FIGURE 5
D_2-hex pencils with: (A) nodal cubics; (B) type (2) cubics.

(d) *C is decomposable: C is a real triangle, real star, triangle with imaginary line-pair, star with imaginary line-pair, one-line-type or two-line-type.*

Proposition 5.2. *A hex pencil contains no cubic with a repeated line (one-line-type or two-line-type), imaginary line-pair (in a triangle or star), or imaginary conic.*

Proof. Let a hex pencil $F : \alpha G + \beta H$ have a curve C with one of the five types just described. The real locus of C consists of one or two lines (or one line and one point). Then 5 of the 9 base points of F must lie on a real line $L \subset C$ (there being at most two). So L meets the triangle G in 5 points, so L is a component of G. But no two cubics in F share a line (otherwise, so do G and H). ∎

In Section 4, we found all types of class (a) represented within D_3 hex pencils $F_{\ell,m}$. Triangles belong to every hex pencil; acnodal cubics and non-singular conic-plus-chords appear in each D_3 hex pencil; a star occurs in the D_6 hex pencil $F_{-1,1}$. In view of Proposition 5.2, it remains only to consider the following four types of singular cubics:

(1) nodal; (2) singular conic-plus-chord; (3) cuspidal; and (4) conic-plus-tangent.

Remark 5.3. If C_0 is one of the types (1)–(4), it cannot appear in a D_3 hex pencil. Unlike the triangle, star, or acnodal cubic, C_0 cannot be made D_3-symmetric, and therefore could only appear in multiples of three. But the discriminant for the D_3-normal form, which may be written as

$$\Delta(c(3x^2y - y^3) - 3a(x^2 + y^2)z + 4bz^3) = bc^2(a^3 - bc^2)^3,$$

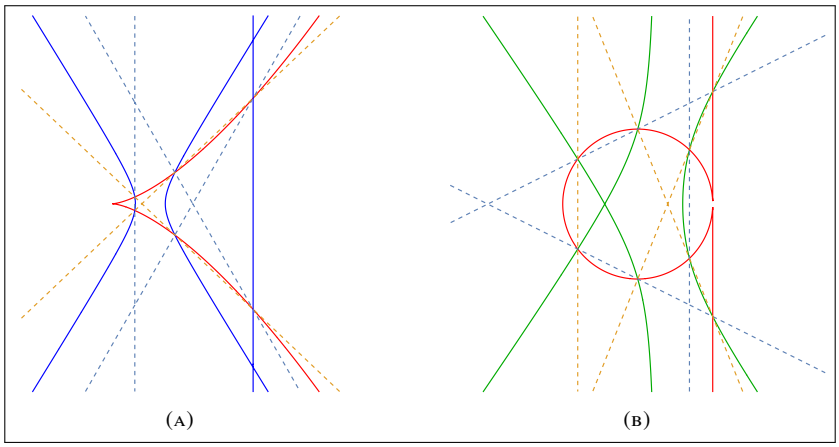

FIGURE 6
Hex pencil with: (A) cusp; (B) conic-plus-tangent.

shows that a D_3-pencil cannot have enough roots of any given type (e.g., three simple roots for three nodal cubics).

In view of the remark, we now turn to hex pencils with less symmetry. Nodal cubics are commonplace in such pencils, as are singular conic-plus-chords in the presence of D_2-symmetry. Figure 5 (A) shows a D_2-symmetrical pencil with a pair of nodes that are exchanged by π-rotations. Figure 5 (B) shows a D_2-symmetrical pencil with a pair of type (2) cubics that are fixed by π-rotations. (The linear component of the blue cubic is the ideal line.)

Our hex pencils with cubics of types (3) and (4) use only reflection symmetry and require more precise constructions; note cusps and conic-plus-tangents are destroyed by small changes in coefficients. For example, for the pencil in Figure 6 (A), the strategy is to *begin* with a cuspidal cubic C, and to construct the triangles so as to meet at 9 points on C. Only 6 such points are visible in the figure. The last step is to choose the third edge of the red triangle to meet the blue triangle three more times on C. A vertical edge does so – twice to the right of the region shown and at the ideal point $(0 : 1 : 0)$. (This pencil happens to contain also a cubic of type (2).)

A similar description applies to Figure 6 (B), which shows the construction of a hex pencil with a conic-plus-tangent (also a nodal cubic, green). In both cases, the method depends on the reflection symmetry of the singular curve.

It is now easy to prove the following result.

Theorem 5.4. *A real cubic belongs to a hex pencil if and only if it has no repeated line, imaginary line-pair, or imaginary conic.*

Proof. The *if* statement is Proposition 5.2. To prove the converse, let C be a real cubic with no repeated or non-real line. Among the examples of this and the previous section, we have found an equivalent cubic $C' \simeq C$ which belongs to a hex pencil $F' : \alpha G' + \beta H'$. A real projective transformation $h \in \mathrm{PGL}(2, \mathbb{R})$ gives $C = h \cdot C'$, so C belongs to the hex pencil generated by $G = h \cdot G'$ and $H = h \cdot H'$. ∎

Remark 5.5. A unified hex pencil construction for cubics (with no repeated or non-real line) should be possible based on the Cayley–Bacharach theorem. Above, we constructed two triangles to meet at 8 points on the given cubic in Figure 6; the existence of a ninth such point was guaranteed by symmetry. For more subtle examples (as in Figure 7 (ɪ), (ᴊ)) the *Cayley–Bacharach theorem* plays the same role. But for a general result, some technical arguments would still be required to produce a pencil which is hexagonal (not just *bi-triangular*).

6. Which of the 279 configurations of Kodaira fibers are hexagonal?

We begin this section by summarizing some topological background which pertains to a pencil of cubics. By limiting the discussion to hex pencils, fortunately, we are able to avoid a number of subtleties which arise in general. Thus, we will quickly get to some concrete questions regarding the connection between hex pencils and the theory of rational elliptic surfaces [8, 9].

For each geometric type of real cubic in a hex pencil, $C \subset \mathcal{HP}$, Table 1 lists the Euler characteristics $\chi(C_{\mathbb{R}})$ and $\chi(C_{\mathbb{C}})$ of the topological subspaces $C_{\mathbb{R}} \subset \mathbb{R}\mathrm{P}^2$ and $C_{\mathbb{C}} \subset \mathbb{C}\mathrm{P}^2$. For example, a non-singular cubic is a circle in $\mathbb{R}\mathrm{P}^2$ or a torus in $\mathbb{C}\mathrm{P}^2$; a nodal cubic is a "figure eight" in $\mathbb{R}\mathrm{P}^2$ or a "pinched torus" in $\mathbb{C}\mathrm{P}^2$; a triangle in $\mathbb{R}\mathrm{P}^2$ has $\chi(C_{\mathbb{R}}) = v - e = -3$; in $\mathbb{C}\mathrm{P}^2$ a triangle consists of three spheres touching pairwise at three points.

The fourth column of the table gives shorthand notation $\chi(C)$ for the pair $\chi(C_{\mathbb{R}})$, $\chi(C_{\mathbb{C}})$ (using bars above integers to denote negative signs). The fifth column gives standard notation for corresponding *Kodaira fibers* resulting from blow up at all 9 base points of the pencil. We observe that the pair $\chi(C)$ for a singular cubic uniquely determines the Kodaira fiber.

Summing over (real) singular curves $C^i_{\mathbb{R}}$ in a hex pencil $\mathcal{HP}$ gives (see [4]):

$$\sum \chi(C^i_{\mathbb{R}}) = \chi(B_9 \mathbb{R}\mathrm{P}^2) = -8. \tag{6.1}$$

Type of real cubic C	$\chi(C_{\mathbb{R}})$	$\chi(C_{\mathbb{C}})$	$\chi(C)$	Fiber
nodal	-1	1	$\overline{1}1$	I_1
acnodal	1	1	11	I_1
cuspidal	0	2	02	II
singular conic + chord	-2	2	$\overline{2}2$	I_2
conic + tangent	-1	3	$\overline{1}3$	III
triangle	-3	3	$\overline{3}3$	I_3
star	-2	4	$\overline{2}4$	IV
non-singular irreducible	0	0	00	I_0
non-singular conic + chord	0	2	02	I_2

Table 1
Data for 9 geometric types of real cubics in hex pencils.

Here, $B_9\mathbb{R}P^2$ is the non-orientable surface obtained from $\mathbb{R}P^2$ by blowing up at the 9 base points p_i, and

$$\chi(B_9\mathbb{R}P^2) = \chi(\mathbb{R}P^2) - 9 = -8,$$

since each p_i is effectively replaced by a circle. The first equality treats $B_9\mathbb{R}P^2$ as a union of disjoint singular curves and *bands* (cylinders or Möbius strips) foliated by the non-singular curves; the bands have $\chi = 0$ and do not contribute to $\chi(B_9\mathbb{R}P^2)$.

Since we view a pencil of real cubics as a singular foliation $\mathcal{F}$ of $\mathbb{R}P^2$, it is natural to interpret equation (6.1) also in terms of the Poincaré–Hopf theorem

$$\sum_{p\in\mathbb{R}P^2} \mathcal{I}_p(\mathcal{F}) = \chi(\mathbb{R}P^2) = 1.$$

The singularities of a curve C in $\mathcal{HP}$ determine singularities of $\mathcal{F}$ (or its tangent line field), whose total contribution to the index sum is $\chi(C_{\mathbb{R}})$. For instance, as Figure 4 illustrates, the three vertices of a triangle C are saddles, contributing $\chi(C_{\mathbb{R}}) = -3$; the isolated singularity of an acnodal cubic C is a center, contributing $\chi(C_{\mathbb{R}}) = 1$; a star gives a singularity of index $\mathcal{I}_p(\mathcal{F}) = \chi(C_{\mathbb{R}}) = -2$. But $\mathcal{F}$ also has 9 "sources" (or "sinks") at the base points of $\mathcal{HP}$. Thus, writing

$$\sum_{p\in\mathbb{R}P^2} \mathcal{I}_p(\mathcal{F}) = \sum \chi(C^i_{\mathbb{R}}) + 9,$$

equation (6.1) may be recovered from the Poincaré–Hopf theorem.

On the other hand, we may consider the sum $\sum \chi(C^i_{\mathbb{C}})$ – not just over real singular cubics in a hex pencil, but also complex ones (these come in conjugate pairs):

$$\sum \chi(C^i_{\mathbb{C}}) = \chi(B_9\mathbb{C}\mathrm{P}^2) = 12. \tag{6.2}$$

This result may be derived by a similar topological argument as in the real case; but in the complex setting, blow up replaces a point by a sphere, thus giving

$$\chi(B_9\mathbb{C}\mathrm{P}^2) = \chi(\mathbb{C}\mathrm{P}^2) + 9 = 12.$$

As in the real case, there is an alternative interpretation of the result which relates more concretely to our examples of pencils of cubics. This is based on the *discriminant form* for a regular pencil of cubics $\mathcal{P} : \alpha G + \beta H : \Delta(\alpha, \beta)$ is a homogeneous polynomial of degree 12 which vanishes exactly when $\alpha G + \beta H$ is singular (as a cubic in $\mathbb{C}\mathrm{P}^2$).

To be brief, an explicit formula for Δ as a 6×6 determinant $\Delta = |M|$ can be given as follows. It can be shown that a singularity p of a cubic F is also singular on its Hessian $H(F) = |D^2 F|$ (see formula for $H(F)$ in [6]). Let M be the 6×6 matrix whose respective rows are formed by the coefficients of the monomials in the six quadrics F_x, F_y, F_z, $H(F)_x$,$H(F)_y$, $H(F)_z$. Then M is singular at p; conversely, it can be shown that M is singular *only* at such points [7].

In particular, this provides a second proof (besides equation (6.2)) that a regular pencil of cubics has at most *twelve* singular curves (in $\mathbb{C}\mathrm{P}^2$): Letting $\delta(C) = \delta(\alpha G + \beta H)$ denote the multiplicity of $(\alpha : \beta)$ as a root of Δ, we have $\sum \delta(C^i) = 12$.

Further, it can be directly verified (by considering the matrix M for representatives of each singular type of cubic [7]) that $\delta(C)$ is precisely the Euler characteristic: $\delta(C) = \chi(C_{\mathbb{C}})$. (Again we assume a hex pencil; the general case is more difficult to state in elementary terms.) Thus, the discriminant provides a computationally useful tool for detecting the (complex) *type* of any singular cubic in $\mathcal{HP}$.

For instance, the discriminant form for the hex pencil in Figure 7 (c) is given by

$$\Delta(\alpha, \beta) = \alpha^3\beta^3(\alpha - \beta)^2(\alpha + \beta)^2(5\alpha^2 + 118\alpha\beta + 5\beta^2).$$

The factors correspond to: Two triangles (red, blue), two singular conic-plus-chords (orange, blue-green), and two acnodes (purple, green); note the last factor has two real roots.

For interpretation of such graphics, which can be intricate, note the following conventions. The generating pair of triangles in Figure 7 are always red and blue (and lines appear as circle-arcs in the disk model $\mathbb{D}^2 \simeq \mathbb{R}\mathrm{P}^2$). All other real singular cubics are shown in other solid colors; non-singular conic-plus-chords appear dashed (these are the only real non-singular cubics which are plotted).

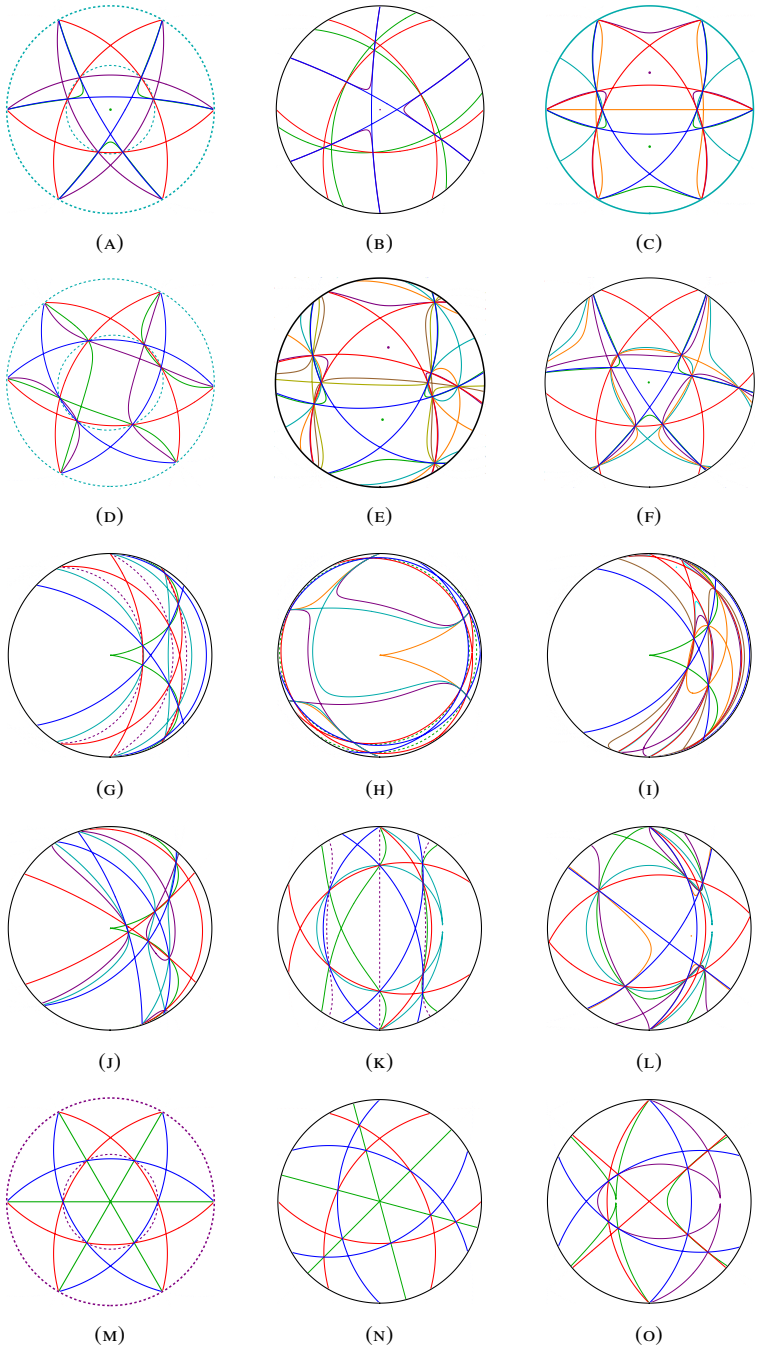

Figure 7
Hex pencils for all but four hex-like configurations.

We now introduce concise notation for tabulation of hex pencils, in Table 2. We begin with the $\mathbb{R}$-*configuration* of a hex pencil, $\mathcal{K}_{\mathbb{R}}(\mathcal{HP})$. This is a list of *all* (real and complex) singular cubics in $\mathcal{HP}$, which makes distinctions related to reality. The type of each C_i is identified by its integer pair $\chi(C_i) = a_i b_i$, and the configuration is given by a sequence of pairs separated by spaces $\mathcal{K}_{\mathbb{R}}(\mathcal{HP}) = a_1 b_1\, a_2 b_2\, \ldots\, a_m b_m$; for brevity, exponents denote repetition of a pair. For example, the two hex pencils in Figure 4 have $\mathbb{R}$-configurations

$$\mathcal{K}_{\mathbb{R}}(F_{-1,1/4}) = \overline{3}3^3\, 11\, 02 \quad \text{and} \quad \mathcal{K}_{\mathbb{R}}(F_{-1,1}) = \overline{3}3^2\, \overline{2}4\, 02.$$

For singular *non-real* cubics (there were none in $F_{-1,1/4}$ and $F_{-1,1}$), we extend our notation $\chi(C) = ab$ using $a = 0$. Pairs for real cubics appear first, followed by $ab = 02$ for a non-singular conic-plus-chord (if it occurs), followed by pairs $0b$ for non-real cubics. The pair $ab = 02$ for a cusp will always precede the pair for another *real* singular cubic (which must exist in a hex pencil). For example, in Figure 6 (A),

$$\mathcal{K}_{\mathbb{R}} = \overline{3}3^2\, 02\, \overline{2}2\, 02.$$

The non-singular conic-plus-chord was not shown in Figure 6, but appears (dashed) in Figure 7 (G), where the same pencil is shown.

The $\mathbb{R}$-configuration $\mathcal{K}_{\mathbb{R}}(\mathcal{HP})$ encodes topological data, in particular, for the corresponding foliation of $\mathbb{R}\mathrm{P}^2$. For example, using Table 2, one may read off the indices of all real singularities and the types of all real singular curves in Figure 7. Now it is reasonable to ask, how fully do these examples represent the range of possible topological behaviors of hex pencil foliations of $\mathbb{R}\mathrm{P}^2$?

For this purpose, we also consider $\mathbb{C}$-*configurations* $\mathcal{K}_{\mathbb{C}}$, or simply *configurations* $\mathcal{K}$, as in the theory of rational elliptic surfaces. With the understanding that every regular pencil of cubics gives rise to such a surface – and in the case of hex pencils we may read off the resulting set of fibers from Table 1 – we may write, e.g., $\mathcal{K}(F_{-1,1/4}) = \mathrm{I}_3^3\, \mathrm{I}_2\, \mathrm{I}_1$ and $\mathcal{K}(F_{-1,1}) = \mathrm{IV}\, \mathrm{I}_3^2\, \mathrm{I}_1^2$. (Roman numerals like IV come first.)

Of course, $\mathcal{K}$ neglects key information pertaining to the foliation of $\mathbb{R}\mathrm{P}^2$. On the other hand, we wish to take advantage of the fact that rational elliptic surfaces are subject to important additional constraints beyond equations (6.1) and (6.2). This is not the place to discuss the role of lattice embeddings, etc., in the more sophisticated theory of surfaces, but the upshot is this: The configuration of a pencil $\mathcal{K}(\mathcal{HP})$ must accordingly be among the 279 fiber configurations determined by Persson [10] and also Miranda [9]. To be clear, all 279 fiber configurations belong to actual elliptic surfaces, and it is also a fact that, to any such surface, there corresponds a pencil of cubics.

But we wish to emphasize that the process of going from a configuration $\mathcal{K}$ to a pencil is far less straightforward than the reverse; more to the point, such a pencil may

Figure 7 (–)	$\mathcal{K}_{\mathbb{R}}(\mathcal{HP})$	$\mathcal{K}_{\mathbb{C}}(\mathcal{HP})$	$\deg(j)$
(A)	$\overline{3}3^3\,11\,02$	$\mathrm{I}_3^3\,\mathrm{I}_2\,\mathrm{I}_1$	12
(B)	$\overline{3}3^3\,11\,01^2$	$\mathrm{I}_3^3\,\mathrm{I}_1^3$	12
(C)	$\overline{3}3^2\,\overline{2}2^2\,11^2$	$\mathrm{I}_3^2\,\mathrm{I}_2^2\,\mathrm{I}_1^2$	12
(D)	$\overline{3}3^2\,\overline{1}1^2\,02\,01^2$	$\mathrm{I}_3^2\,\mathrm{I}_2\,\mathrm{I}_1^4$	12
(E)	$\overline{3}3^2\,11^2\,\overline{1}1^4$	$\mathrm{I}_3^2\,\mathrm{I}_1^6$	12
(F)	$\overline{3}3^2\,11\,\overline{1}1^3\,01^2$	$\mathrm{I}_3^2\,\mathrm{I}_1^6$	12
(G)	$\overline{3}3^3\,02\,\overline{2}2\,02$	$\mathrm{II}\,\mathrm{I}_3^2\,\mathrm{I}_2^2$	10
(H)	$\overline{3}3^2\,02\,\overline{1}1^2\,02$	$\mathrm{II}\,\mathrm{I}_3^2\,\mathrm{I}_2\,\mathrm{I}_1^2$	10
(I)	$\overline{3}3^2\,02\,11\,\overline{1}1^3$	$\mathrm{II}\,\mathrm{I}_3^2\,\mathrm{I}_1^4$	10
(J)	$\overline{3}3^2\,02\,\overline{1}1^2\,01^2$	$\mathrm{II}\,\mathrm{I}_3^2\,\mathrm{I}_1^4$	10
(K)	$\overline{3}3^2\,\overline{1}3\,\overline{1}1\,02$	$\mathrm{III}\,\mathrm{I}_3^2\,\mathrm{I}_2\,\mathrm{I}_1$	9
(L)	$\overline{3}3^2\,\overline{1}3\,11\,\overline{1}1^2$	$\mathrm{III}\,\mathrm{I}_3^2\,\mathrm{I}_1^3$	9
(M)	$\overline{3}3^2\,\overline{2}4\,02$	$\mathrm{IV}\,\mathrm{I}_3^2\,\mathrm{I}_2$	8
(N)	$\overline{3}3^2\,\overline{2}4\,01^2$	$\mathrm{IV}\,\mathrm{I}_3^2\,\mathrm{I}_1^2$	8
(O)	$\overline{3}3^2\,\overline{1}3^2$	$\mathrm{III}^2\,\mathrm{I}_3^2$	6

Table 2
Hex pencils configurations for Figure 7.

or may not be real, and when it is, it may not be topologically unique as a foliation of $\mathbb{R}\mathrm{P}^2$. (For example, Table 2 shows that (E) and (F) are *pencil isomers* [7]; likewise (I) and (J).) Thus, one cannot expect a *classification* of real cubic pencil foliations of $\mathbb{R}\mathrm{P}^2$ to fall directly out of the theory of elliptic surfaces.

On the other hand, considering the relative topological simplicity of hex pencils, such a goal may not be unreasonable for this special class. Note that a configuration $\mathcal{K}(\mathcal{HP})$ must have a term I_3^2 or I_3^3. (Note that $\mathcal{K} = \mathrm{I}_3^4$ identifies the equivalence class of the Hessian pencil, which is not a hex pencil!) Perusing the list in [9] (which uses abbreviated notation $\mathrm{I}_3^2 = 3^2$, $\mathrm{I}_3^3 = 3^3$, etc.), one finds that there are only 17 such *hex-like configurations*.

Which brings us to the question:

> *Of the* 17 *hex-like configurations in the list of* 279*, which ones are actually realized by hex pencils, and what are all the possible topological types of the resulting foliations of* $\mathbb{R}\mathrm{P}^2$*?*

In fact, we observe that the examples listed in Table 2 realize all but four of the 17 hex-like configurations. One of the four is easy to dismiss: $\mathcal{K} = \mathrm{II}^3\,\mathrm{I}_3^2$ is consistent only

with a hex pencil with 1 or 3 real cusps; but since a cusp has $\chi(C^i_{\mathbb{R}}) = 0$, such a pencil would in any case result in the sum $\sum \chi(C^i_{\mathbb{R}}) = -6$, contradicting equation (6.1). So only the following three configurations are in doubt:

$$\mathcal{K} = \mathrm{II}^2\,\mathrm{I}_3^2\,\mathrm{I}_2, \quad \mathcal{K} = \mathrm{II}^2\,\mathrm{I}_3^2\,\mathrm{I}_1^2, \quad \mathcal{K} = \mathrm{III}\,\mathrm{II}\,\mathrm{I}_3^2\,\mathrm{I}_1.$$

In the first two of these, the cusps might come in complex conjugate pairs, which would be rather disappointing for the foliation of $\mathbb{R}\mathrm{P}^2$! Thus, we leave off with the open question: *Is there a hex pencil with two real cusps?*

References

[1] M. Artebani and I. Dolgachev, The Hesse pencil of plane cubic curves. *Enseign. Math. (2)* **55** (2009), no. 3-4, 235–273. Zbl 1192.14024 MR 2583779

[2] A. Bonifant and J. Milnor, On real and complex cubic curves. *Enseign. Math.* **63** (2017), no. 1-2, 21–61. Zbl 1390.14088 MR 3777131

[3] E. Brieskorn and H. Knörrer, *Plane algebraic curves*. Mod. Birkhäuser Class., Birkhäuser, Basel, 1986. Zbl 0588.14019 MR 2975988

[4] A. I. Degtyarev and V. M. Kharlamov, Topological properties of real algebraic varieties: Rokhlin's way. *Uspekhi Mat. Nauk* **55** (2000), no. 4(334), 129–212. Zbl 1014.14030 MR 1786731

[5] C. G. Gibson, *Elementary geometry of algebraic curves: An undergraduate introduction*. Cambridge University Press, Cambridge, 1998. Zbl 0997.14500 MR 1663524

[6] F. Kirwan, *Complex algebraic curves*. London Math. Soc. Stud. Texts 23, Cambridge University Press, Cambridge, 1992. Zbl 0744.14018 MR 1159092

[7] J. Langer and J. Wall, On foliations of the real projective plane defined by decomposable pencils of cubics. *J. Geom.* **113** (2022), no. 1, article no. 13. Zbl 1492.14009 MR 4373448

[8] R. Miranda, *The basic theory of elliptic surfaces*. Dottorato di Ricerca in Matematica., ETS, Pisa, 1989. Zbl 0744.14026 MR 1078016

[9] — Persson's list of singular fibers for a rational elliptic surface. *Math. Z.* **205** (1990), no. 2, 191–211. Zbl 0722.14022 MR 1076128

[10] U. Persson, Configurations of Kodaira fibers on rational elliptic surfaces. *Math. Z.* **205** (1990), no. 1, 1–47. Zbl 0722.14021 MR 1069483

(Reçu le 29 juillet 2021)

Joel Langer, Department of Mathematics, Case Western Reserve University, Cleveland, 44106-7058, USA; *e-mail:* joel.langer@case.edu

Jeremy Wall, Department of Mathematics, Case Western Reserve University, Cleveland, 44106-7058, USA; *e-mail:* jeremy.wall@case.edu